Article:
Aruffo, E, Di Carlo, P, Dari-Salisburgo, C et al. (20 more authors) (2014) Aircraft observations of the lower troposphere above a megacity: Alkyl nitrate and ozone chemistry. Atmospheric Environment, 94. pp. 479-488. ISSN 1873-2844

https://doi.org/10.1016/j.atmosenv.2014.05.040

Accepted Manuscript

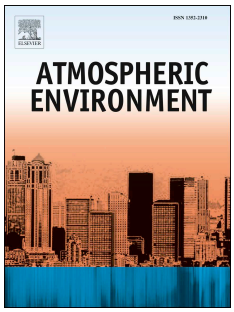

Aircraft observations of the lower troposphere above a megacity: alkyl nitrate and ozone chemistry

Eleonora Aruffo , Piero Di Carlo , Cesare Dari-Salisburgo , Fabio Biancofiore , Franco Giammaria , Marcella Busilacchio , James Lee , Sarah Moller , James Hopkins , Shalini Punjabi , Stephane Bauguitte , Debbie O'Sullivan , Carl Parcival , Michael Le Breton , Jennifer Muller , Rod Jones , Grant Forster , Claire Reeves , Dwayne Heard , Hannah Walker , Trevor Ingham , Stewart Vaughan , Daniel Stone

PII: S1352-2310(14)00387-2

DOI: 10.1016/j.atmosenv.2014.05.040

Reference: AEA 12984

To appear in: *Atmospheric Environment*

Received Date: 5 December 2013

Revised Date: 12 May 2014

Accepted Date: 14 May 2014

Please cite this article as: Aruffo, E., Di Carlo, P., Dari-Salisburgo, C., Biancofiore, F., Giammaria, F., Busilacchio, M., Lee, J., Moller, S., Hopkins, J., Punjabi, S., Bauguitte, S., O'Sullivan, D., Parcival, C., Le Breton, M., Muller, J., Jones, R., Forster, G., Reeves, C., Heard, D., Walker, H., Ingham, T., Vaughan, S., Stone, D., Aircraft observations of the lower troposphere above a megacity: alkyl nitrate and ozone chemistry, *Atmospheric Environment* (2014), doi: 10.1016/j.atmosenv.2014.05.040.

Aircraft observations of the lower troposphere above a megacity: alkyl nitrate and ozone chemistry

Eleonora Aruffo[1,2], Piero Di Carlo[1,2], Cesare Dari-Salisburgo[1], Fabio Biancofiore[1,2], Franco Giammaria[2], Marcella Busilacchio[1], James Lee[3], Sarah Moller[3], James Hopkins[3], Shalini Punjabi[3], Stephane Bauguitte[4], Debbie O'Sullivan[5], Carl Parcival[6], Michael Le Breton[6], Jennifer Muller[6], Rod Jones[7], Grant Forster[8], Claire Reeves[8], Dwayne Heard[9,10], Hannah Walker[9], Trevor Ingham[9,10], Stewart Vaughan[9], Daniel Stone[9]

[1]Center of Excellence CETEMPS Universita' degli studi di L'Aquila, Via Vetoio, 67010 Coppito, L'Aquila, Italy

[2]Dipartimento di Scienze Fisiche e Chimiche, Universita' degli studi di L'Aquila, Via Vetoio, 67010 Coppito, L'Aquila, Italy

[3]Departement of Chemistry, University of York, UK

[4]FAAM, Cranfileld University, UK

[5]Observation Based Reasearch (OBR), Met Office, FitRoy Road Exeter EX1 3PB, UK

[6]School of Earth, Atmospheric and Environmental Science, The University of Manchester, UK

[7]Department of Chemistry, University of Cambridge, UK

[8]School of Environmental Sciences, University of East Anglia, UK

[9]School of Chemistry, University of Leeds, UK

[10] National Centre for Atmospheric Science, University of Leeds, UK

Corresponding author: Eleonora Aruffo, Dipartimento di Scienze Fisiche e Chimiche, Universita' degli studi di L'Aquila, Via Vetoio, 67010 Coppito, L'Aquila, Italy, +390862433084, e-mail: eleonora.aruffo@aquila.infn.it.

Abstract

Within the framework of the RONOCO (ROle of Nighttime chemistry in controlling the Oxidising Capacity of the atmOsphere) campaign a daytime flight over the metropolitan area of London were carried out to study the nitrogen oxide chemistry and its role in the production and loss of ozone (O_3) and alkyl and multifunctional nitrate (ΣANs). The FAAM BAe-146 aircraft, used for these observations, was equipped with instruments to measure the most relevant compounds that control the lower troposphere chemistry, including O_3, NO, NO_2, NO_3, N_2O_5, HNO_3, peroxy nitrates (ΣPNs), ΣANs, OH, and HO_2. In the London's flight a strong ozone titration process was observed when flying above Reading (downwind of London) and when intercepting the London plume. The coupled cycles of NO_x and HO_x can have different terminations forming ΣPNs, ΣANs, HNO_3 or peroxides (H_2O_2, ROOH) altering the O_3 production. In the observations reported here, we found that a strong ozone titration (ΔO_3 = -16 ppb), due to a rapid increase of NO_x (ΔNO_x = 27 ppb), corresponds also to a high increase of ΣANs concentrations ($\Delta\Sigma ANs$ = 3 ppb), and quite stable concentrations of HNO_3 and ΣPNs. Unexpectedly, compared with other megacities, the production of ΣANs is similar to that of O_x (O_3 + NO_2), suggesting that in the London plume, at least during these observations, the formation of ΣANs effectively removes active NO_x and hence reduces the amount of O_3 production. In fact, we found that the ratio between the ozone production and the alkyl nitrates production (observed) approximate the unity; on the contrary the calculated ratio is 7. In order to explain this discrepancy, we made sensitivity tests changing the alkyl nitrates branching ratio for some VOCs and we investigated the impact of the unmeasured VOCs during the flight, founding that the calculated ratio decreases from 7 to 2 and that, in this condition, the major

contribution to the *ΣANs* production is given by Alkanes. Observations and analysis reported here suggest that in the London plume the high NO_x emissions and the chemistry of some VOCs (mainly Alkanes) produce high concentrations of *ΣANs* competing against the local ozone production.

Highlights

- Daytime chemical and aerosol composition have been measured around London with an aircraft
- Unexpected high production of alkyl nitrate comparable to that of ozone
- The low O_3 production put the chemistry above London quite different compared with other megacities

Keywords

Ozone production; alkyl nitrates production; tropospheric chemistry; urban pollution; aircraft; London.

1. Introduction

NO_x ($NO_x = NO + NO_2$), produced principally as NO by human activity (transport, industrial combustion, etc.), and O_3 are significant tropospheric pollutants that can have negative impact on the vegetation, ecosystems and human health (e.g. European Environment Agency (EEA), 2005). In recent years the scientific community has paid considerable attention to the study of the chemical and physical mechanisms that control the chemistry of nitrogen compounds in the troposphere, focusing in detail on NO_x and the total reactive oxidized nitrogen species, NO_y ($NO_y = NO_x + NO_z$, where $NO_z = RO_2NO_2 + RONO_2 + HNO_3 + HONO + 2N_2O_5 + NO_3$). Some of the NO_z compounds are a sink for NO_x (for example HNO_3), whereas other are a temporary reservoirs of NO_x in the troposphere and therefore their formation can enhance ozone production if the NO_x is released

downwind into a low NO_x environment (e.g. Jacob et al, 1999; Day et al., 2002). In the troposphere, the termination of coupled cycles of NO_x and HO_x ($HO_x = OH + HO_2$) has been studied in detail in recent years due to their impact on peroxy nitrates (ΣPNs), alkyl and multifunctional nitrates (ΣANs) and O_3 formation. When a hydrocarbon (RH) is oxidised by OH, a peroxy radical (RO_2) is formed, which can react with NO forming either an alkyl nitrate (R2) or alkoxy radical RO (R3), the latter lead the production of NO_2 and therefore, after its photolysis, produces two molecules of O_3.

$$OH + RH + O_2 + M \rightarrow RO_2 + H_2O + M \quad \text{(R1)}$$

$$RO_2 + NO + M \rightarrow RONO_2 + M \quad \text{(R2)}$$

$$RO_2 + NO \rightarrow RO + NO_2 \quad \text{(R3)}$$

$$RO + O_2 \rightarrow R'C(O) + HO_2 \quad \text{(R4)}$$

$$HO_2 + NO \rightarrow OH + NO_2 \quad \text{(R5)}$$

$$2NO_2 + 2h\nu \rightarrow 2NO + 2O \quad \text{(R6)}$$

$$2O + 2O_2 + 2M \rightarrow 2O_3 + 2M \quad \text{(R7)}$$

The urban environments are very interesting and well investigated from the point of view of air quality because of intense human activities that characterize these areas. Different campaigns have been carried out in the London metropolitan area. The results of the REPARTEE (REgents PARk and Tower Environmental Experiment) project have been presented by Harrison et al. (2012). They showed the chemical and physical mechanisms controlling the London atmosphere and introduced a history of London air quality problems: for example, in consequence of the Great Smog in 1952, more than 4000 excess deaths have been estimated. In contrast to what was observed in other important megacities, such as Mexico City or Los Angeles, Charron et al. (2007) found that a large fraction of the particulate matter (PM10) measured in London derived from regional backgrounds. This result suggests that in depth study of the atmospheric composition in urban areas and the

93 regional background around London is therefore important (Harrison et al., 2012). During the
94 REPARTEE study, a collaboration with the CityFlux experiment (Langford et al., 2010) was
95 established to carry out measurements of Volatile Organic Compounds (*VOCs*) and aerosols fluxes
96 and chemical compositions in different urban areas of London. They found that the traffic emissions
97 contribute for more than 70% of the aromatic compounds and in general are the principal source of
98 *VOCs* in the London plumes. The study of the *VOCs* fluxes and concentrations by Langford et al.
99 (2010) shows that their observations are in agreement with the measurements of the UK NAEI
100 (National Atmospheric Emission Inventory) for aromatic *VOCs*. In contrast for the species emitted
101 by several and diffuse area sources (as acetaldehyde or acetone, produced also by paints, solvents
102 etc.) the emission inventory underestimates the observations of Langford et al. (2010).
103 McMeeking et al. (2012) presented the results of their measurements during the EM25 (Emissions
104 around the M25 motorway) campaign (June 2009) in London. They identified the London plume
105 with respect to the regional background, measuring different concentrations of the most significant
106 compounds emitted in the urban area (NO_x, *CO*, some *VOCs* and black carbon (*BC*)) flying within
107 or outside the city plume and characterized the two air masses by composition and age. They
108 studied the aerosol mass distribution, finding little difference between the urban plume and the
109 regional aerosol. The two case studies reported in their work show that the London plume advected
110 west for the flight on 23 June 2009, characterized by easterly flow, and remained over London for
111 the more stagnant 22 June 2009 flight. Moreover, during the flight of 23 June the NO_x concentration
112 measured above Reading was significantly high, reach the maximum value of about 30 ppb. As a
113 consequence of the high NO_x concentration over Reading, they reported a decreasing ratio between
114 O_3 and NO_x as low as close to zero indicating a significant ozone titration processes in the London
115 plumes.
116 As previously illustrated, an interesting aspect of the tropospheric chemical mechanisms within the
117 urban and suburban environments is the balance between the alkyl nitrates and the ozone production

in the NO_x-HO_x coupled cycles (R1-R7 reactions); its implications for the chemical composition of the troposphere have been investigated by several authors in different urban environments. Rosen et al. (2004) measured *ΣANs* during the Texas Air Quality Study in 2000 (TexAQS-2000) at La Porte and calculated the ratio between the ozone production and the *ΣANs* production finding slopes of ΔOx/ΔANs between 29 and 41 that implies a high yield (between 0.065 and 0.047) for alkyl nitrate. Perring et al. (2010) investigated the production of the *ΣANs* in the Mexico City plume finding that the alkyl nitrates play a significant role in the photochemistry of this urban site since they observed that *ΣANs* was 10-20% of the NO_y and its formation suppresses peak ozone production rates by about 40% . Farmer et al. (2011) used a model and data observed in Mexico City to point out the role of alkyl nitrates in the photochemistry of the lower troposphere: they showed that *ΣANs* production can affect the O_3 production. This has implications on the dependence of O_3 production on NO_x and *VOCs* and therefore on designing air quality control strategies since current chemical mechanisms included in urban and regional air quality models omit details of the alkyl nitrates production.

The RONOCO (Role of Nighttime chemistry in controlling the Oxidising Capacity of the AtmOsphere) project was carried out to investigate the nocturnal chemistry around the UK during different seasons, with particular attention given to the role of the nitrate radical. In this framework, two airborne campaigns were carried out during July-September 2010 and January 2011. The principal deliverables of the project are: 1) comprehensive measurements of nighttime radicals, their sources and sinks, and aerosol composition in the boundary layer and free troposphere in a range of conditions; 2) quantification of the key processes that control nighttime chemical processes; 3) assessment of the impacts of nighttime chemistry on regional scales; 4) an assessment of the global impacts of nighttime chemistry in the current and future atmospheres (Stone et al., 2013).

In this paper we analyse the observations carried out on-board the BAe-146 aircraft during a daytime flight along the M25 motorway around the megacity of London. The flight consists of three runs with a very similar path to follow the M25 motorway. Here the simultaneous measurements of compounds not observed in McMeeking et al. (2012), like *ΣPNs*, *ΣANs* and HNO_3 can help a further understanding of the chemistry around London. The main goal is to investigate the role of NO_x and NO_y in the ozone budget of this area.

2. Instrumental

The observations that will be presented in this work were carried out aboard the UK BAe 146-301 atmospheric research aircraft of the Facility for Airborne Atmospheric Measurements (FAAM). During the RONOCO campaign several instruments were fitted on the BAe-146-301 aircraft, but here only the instruments from which data are used in the analysis are described. NO_2, *ΣPNs* and *ΣANs* were measured using the TD-LIF (Thermal Dissociation – Laser Induced Fluorescence) instrument developed at the University of L'Aquila (Italy). Briefly, the TD-LIF light source is a pulsed YAG-laser (Spectra-Physics, model Navigator I) that emits light at 532 nm with a power of 3.8 W, a repetition rate of 15 kHz. The laser beam is steered by two high reflectivity mirrors (99%) before entering the first detection cell through a 5 cm diameter window, and leaves the other side of the cell through another antireflection window. In this configuration the laser radiation is sent sequentially through four cells: after each cell the beam is steered into the subsequent cell using high reflectivity mirrors. The laser power is monitored before and after each cell by four photodiode detectors (UDT55) to compensate the fluorescence counts for the laser power changes. In the first cell is measured directly NO_2, whereas *ΣPNs*, *ΣANs* and HNO_3 are thermally convert into NO_2 and measured as difference between the NO_2 detected by adjacent cells (Day et al., 2002; Di Carlo et al., 2013). The conversion temperatures, in the RONOCO configuration, were 200°C, 400°C and 550°C for *ΣPNs*, *ΣANs* and HNO_3, respectively. Ambient air is sampled through a common inlet (a PFA

tube of 120 cm, 6.4 mm OD and 3.8 mm ID) at a flow rate of ~8.4 l/min and, subsequently, it is split into 4 equal flows to pass through four U-shaped quartz tubes (60 cm length, 6 mm OD, 3.8 mm ID). The first quartz tube is not heated because goes to the NO_2 cell, whereas the other are heated at the 3 distinct temperatures reported above to measure in the last three distinct cells *ΣPNs*, *ΣANs* and HNO_3, respectively. The TD-LIF is calibrated using a mixture of high purity zero air and a NIST traceable NO_2. The detection limits of the TD-LIF, in the RONOCO configuration, are: 9.8 pptv, 18.4 pptv, 28.1 pptv and 49.7 pptv (1 s, S/N = 2) for detection of NO_2 by the NO_2 cell, ∑*PNs* cell, ∑*ANs* cell and HNO_3 cell, respectively. The accuracy depends on the uncertainty of the standards and mass flow controller used for the calibration and in this configuration is 10%, 22%, 34% and 46% for NO_2 cell, ∑*PNs* cell, ∑*ANs* cell and HNO_3 cell, respectively. More information about the TD-LIF system, its controller and the calibration system can be found in Di Carlo et al. (2013) and Dari Salisburgo et al. (2009).

The measurements of O_3 and *CO* were made using a standard TECO 49C UV photometric instrument and an UV fluorescence Aero-Laser AL5002 instrument, respectively (FAAM instruments). Detailed information about the technique and the calibration procedures of those analyzers can be found elsewhere (Hopkins et al., 2011).

A chemiluminescent instrument was also used to measure the NO_x (FAAM instrument); in this method ambient *NO* reacts with O_3 generated by the instrument, to produce electronically excited NO_2, which relaxes and emits a photon. The concentration of *NO* is directly measured detecting the chemiluminescence light emitted by the excited NO_2. Ambient NO_2 is detected after a photolytically conversion (using a blue-light LED, centred at 395 nm) into *NO* (Sadanaga, et al., 2010).

In order to measure *VOCs* concentrations a WAS (Whole Air Sampling) coupled to a GC-FID (Gas Chromatography Flame Ionization Detector) (University of York) instrument was used. The WAS system consists of sixty four silica passivated stainless steel canisters of three litres internal volume (Thames Restek, UK) fitted to the rear hold of the aircraft (Hopkins et al., 2002, 2011).

OH and HO_2 were measured by the University of Leeds aircraft FAGE (Fluorescence Assay by Gas Expansion) instrument. The instrument samples ambient air through a pinhole which extends through a window blank in the aircraft, and the gas flows through low-pressure (~1.8 Torr) detection cells for *OH* and HO_2 in series. *OH* is detected by laser-induced fluorescence spectroscopy, in which the radical is electronically excited by laser light at $\lambda \sim 308$ nm. HO_2 is detected in the downstream cell following conversion to *OH* with an excess of *NO*. During RONOCO, the detection cell pressure varied from 1.2 Torr at 6 km to 1.9 Torr at sea level. The limits of detection for *OH* and HO_2 during flight B536 were 1.8×10^6 and 6.9×10^5 molecule cm^{-3}, and during flight B548 were and 1.2×10^6 and 5.9×10^5 molecule cm^{-3} (Commane et al., 2010; Stone et al., 2011; Stone et al., 2013).

Nitric acid and ammonia were measured using a CIMS (Chemical Ionisation Mass Spectrometry) (University of Manchester); in this method the molecules are charged (soft ionization to form little ion fragmentation) and then detected by a mass spectrometer (Le Breton et al., 2012; Von Bobrutzki et al., 2010).

3. Observations

The flight of the RONOCO campaign (B548) selected for this analysis has been chosen in order to examine the London urban plume. The flight followed the route of the M25, a very busy and congested 188 km long motorway that circumnavigates Greater London. The B548 flight was a diurnal flight, carried out on 3 September 2010; the take-off occurred at 09:55 UTC, and after

running along the east coast of the UK made three anticlockwise M25 circuits at about 660 m of altitude during which two missed approaches were made at Northolt (at about 11:35 UTC) and Southend airports (at about 11:55 UTC). The landing occurred at 14:10 UTC. Fig. 1 shows the flight track with the altitude. Analyzing the land use (figure not reported here) in the London urban -suburban region and Reading, it is expected that the chemical processes that are relevant to the troposphere in those regions are those typical of the urban and industrial environments.

The meteorological conditions which occurred during the flight can be derived analysing the 500 hPa geopotential height and the isobars field (NCEP reanalyzed data by www.wetterzentrale.de) and the soundings observations (data available at http://weather.uwyo.edu/upperair/sounding.html - Department of Atmospheric Science – University of Wyoming, USA), figures not showed here. The B548 flight was characterized by a high pressure system over the UK: a wind field from North-East is established over the central UK and London with weak intensity of about 5 knots and blue sky (confirmed by the Nottingham balloon soundings (figure not reported here)).

4. Data analysis

4.1 Data overview

Fig. 2 shows the time series of NO_x (NO_2 measured by the TD-LIF instrument and NO by the chemiluminescent), ΣANs (measured by TD-LIF), CO (measured by Aero Laser), O_3 (measured by TECO), O_x ($O_3 + NO_2$) and altitudes.

Three large plumes of NO_x and CO, observed flying at constant altitude and well below the boundary layer, are easily identifiable (Fig. 2). The PBL height was checked during the flight doing a profile with the aircraft before starting the three runs around London: the meteorological and chemical measurements confirmed the PBL level. During the flight, the wind blew in an easterly direction from the North Sea inland (see Fig. 3), so that the west London region was downwind from London so it is likely to have experienced transport of pollutants from London during the morning rush hour. Moreover, the peak of the three plumes was measured each time the aircraft

240 flew over Reading (at constant altitude), a city in the county of Berkshire, where the NO_x reached
241 the maximum concentrations of about 30 ppb. Fig. 3 shows the NO_2 detected by the aircraft around
242 London area (upper panel) relative to each run along the M25: it is evident that during the flight
243 NO_2 concentrations are higher in the West London region (especially above Reading). In the bottom
244 panel of Fig. 3 the wind direction measured during the flight (black arrows) and the NO_2
245 concentration measured in three ground stations (H: Haringey, L: London and R: Reading) are
246 shown for each M25 run; it is possible to deduce that the NO_2 measured on the ground and that
247 measured in flight show similar features, with lower concentrations at Haringey and higher at
248 Reading.
249 As a result of the NO_x plumes a significant ozone titration phenomenon is found, with a strong O_3
250 reduction (ΔO_3 = -16 ppb) reaching ~20 ppb (Fig. 2), the lowest value observed during the whole
251 flight. During the O_3 titration, a substantial increase of the ΣANs concentration was observed: the
252 increase measured was of about $\Delta\Sigma ANs$ = 3 ppb (maximum value of ~3.5 ppb), probably due to the
253 local emissions of NO_x (Reading) and those transported from London. The high NO_x concentrations
254 above Reading, observed here, are in agreement with what observed by McMeeking et al. (2012), in
255 their flight above the M25 in June 2009. They measured similar concentrations of NO_x (about 30
256 ppb) and a ratio between O_3 and NO_x that decreases until the lowest concentration (around zero)
257 indicating a significant ozone titration processes in the London plumes, as found in our analysis.
258 Besides the analogously observed above Reading the flight studied in this work present similar
259 conditions of the flight of June 2009 reported by McMeeking et al. (2012) also in respect of the
260 highest concentrations measured in the West London region and wind flowing easterly. Here the
261 simultaneous measurements of compounds not observed in McMeeking et al. (2012), like ΣPNs,
262 ΣANs and HNO_3 can help a further understanding of the chemistry around London focusing on the
263 O_3 budget (see below, section 4.3).
264

4.2 Photochemical age: flight B548

In this work we estimated the photochemical age of the air for the daytime diurnal flight B548 using both qualitative and quantitative methods. The ratio between NO_x and HNO_3 can be used as an approximate indication of the photochemical process state: it is expected that the ratio would decrease with increasing plume age (Perring et al., 2010). From the time series of the NO_x/HNO_3 ratio (figure not reported here) two areas can be identified: East and West London regions, corresponding to those described in the paragraph 4.1. The qualitative photochemical process state estimation suggests that West London is impacted by relatively young air masses emitted locally. NO_x is emitted mainly as NO that reacts with ozone to form NO_2, reaching equilibrium rapidly; during the daytime NO_x can be oxidized by OH, producing HNO_3, or can react with RO_2 producing ΣPNs and ΣANs. The NO_y, therefore, is an indicator of the NO_x oxidation. Consequently, the ratio between NO_x and NO_y allows discrimination between fresh air and more aged air that is representative of more regional air mass (the NO_x/NO_y ratio decreases, with increasing NO_x oxidation).

Using the NO_x/NO_y ratio it is possible also to quantitatively estimate the photochemical age Δt that can be defined as (Kleinman et al., 2008; Slowik et al., 2011):

$$\frac{dNO_x}{dt} = k_{NO_x+OH}[NO_x][OH]$$

$$\int \frac{dNO_x}{NO_x} = \int k_{NO_x+OH}[OH]dt$$

$$\frac{[NO_x]_t}{[NO_x]_0} = \exp\left(-k_{NO_x+OH}[OH]\Delta t\right) \quad (1)$$

To evaluate NO_x at time zero, we assume that all NO_y originates as NO_x ($[NO_x]_0 = [NO_y]$) (Kleinman et al., 2008; Slowik et al., 2011) and equation (1) can be written as:

$$\Delta t = -\ln\left(\frac{[NO_x]_t}{[NO_y]}\right)\frac{1}{k_{NO_x+OH}[OH]} \quad (2)$$

284

285 For this analysis we used the mean *OH* concentration measured by the FAGE instrument during the
286 M25 circuits, giving $[OH]$=1.77×10^6 molecules cm^{-3}. In Fig. 4 the values of the term
287 $-\ln([NO_x]_t/[NO_y])$ (at the top) and the photochemical ages (at the bottom) of the air masses
288 sampled during the B548 flight are shown. The $-\ln([NO_x]_t/[NO_y])$ term increases as the air
289 masses become older and confirms the presence of two regimes (East and West London). As
290 expected, the photochemical age is lower (ranging between 2 and 10 hr and a mean value of about 5
291 hr) over the West London region that is a downwind of London area and over Reading (see Fig. 3)
292 indicating that a fresh air plume originated in the London metropolitan area during the rush hour
293 was advected to the west possibly taking in fresh emissions from urban areas on route (i.e. Reading
294 town emissions).
295 In Fig. 5 (upper panel) the trends of the concentrations of *NO_x*, *ΣPNs*, *ΣANs* and *HNO_3* measured
296 along the M25 motorway as a function of the photochemical age calculated using equation (2) are
297 shown. As expected, increasing the age of the plume decreases the *NO_x* level in favour of an
298 increase of its oxidation products. Fig. 5 (lower panel) shows the dependence of the *NO_y* speciation
299 on the photochemical age: the *HNO_3* contribution to the *NO_y* increases in aged plumes and
300 represents the principal *NO_x* reservoir (the *NO_x/NO_y* decreases from 0.81 to 0.32 (from 3 to 19 hours
301 of aging); the *HNO_3/NO_y* increases from 0.13 up to 0.33 and the *$\Sigma ANs/HNO_3$* increases from 0.08 up
302 to 0.26).
303 In several studies the photochemical age of air masses has been estimated using *VOC*s ratios
304 (Kleinman et al., 2003; Liggio et al., 2010). Briefly, the photochemical age was based on
305 differential gas phase reaction rates of toluene and benzene with the *OH* radical. The concentration

306 of the toluene resulting from *OH* oxidation can be calculated as a function of time ($C_T(t)$) (Liggio
307 et al., 2010):
308

$$C_T(t) = C_T(0)\exp(-k_T[OH]t) \quad (3)$$

309
310 where $C_T(0)$ represents the initial concentration of the toluene and k_T the kinetic rate constant
311 between toluene and *OH*. Using an equation similar to equation 3 for benzene, it is possible to
312 evaluate its concentration at time *t* ($C_B(t)$); the ratio between the estimated concentrations of
313 benzene and toluene ($R_{T/B} = C_T(t)/C_B(t)$) can be used to calculate the photochemical age of air
314 masses:

$$AGE = \frac{\ln\left(\frac{R_{T/B}(t)}{R_{T/B}(0)}\right)}{(k_B - k_T)[OH]} \quad (4)$$

315
316 In our analysis, we cannot use this method because we do not have an initial concentration of
317 toluene ($C_T(0)$) and benzene ($C_B(0)$) in order to calculate the age; but we can generate, using the
318 lagrangian Hysplit model (Draxler et al., 2003), the back trajectories starting from a point along the
319 flight trajectory (point R - Reading in Fig. 1) and understanding where the air mass was 5 hours
320 before it was sampled. The air masses reach the area with highest NO_x (point R in Fig. 1 - above
321 Reading - West London) at 11:00 UTC having come from over the London area earlier (air masses
322 coming from a point in the center of the M25 circle, which is the London metropolitan area, at
323 07:00 UTC). At point R (Fig. 1) the concentration of the toluene measured during the B548 flight
324 was about 390 ppt (similar to the other values of toluene measured in the high NO_x area); we did a
325 qualitative test to estimate which concentration of toluene should have been in point in the center of
326 the M25 circle in order to measure 390 ppt of toluene in the point R, that is Reading in Fig. 1 (after
327 5 hours). We found that the estimated $C_T(0)$ is about 460 ppt; Langford et al. (2010), between 20th

and 30th October 2006, measured concentrations of toluene on the Telecom tower (London) in the range of ~200 and ~1800 ppt, it is possible, therefore, to deduce that the estimated $C_T(0) \approx 460$ ppt is a credible value above London. Consequently, the estimation of 5 hours for the age of the air mass is reasonable. McMeeking et al. (2012) calculated the photochemical age of the air masses around London using the ratio between benzene and toluene, commonly used for this analysis because of the different lifetimes of those species. In the London plume (downwind region, West London) they found low benzene/toluene ratios and elevated pollutant concentrations corresponding to fresh emissions, in other regions they measured high benzene/toluene ratios suggesting more aged regional pollution or aged plumes from non-London sources. During RONOCO (B548 flight) the ratio between toluene and benzene increases in the East London region and decreases in the London plume side confirming the distinction between West and East London regions. In Fig. 6, the benzene to toluene ratio and the O_3/NO_x ratio are shown: in respect to the East London region the increase in the ratio between the two volatile organic compounds indicates more aged regional air masses and the increase in O_3/NO_x implies a major level of the ozone concentrations; in contrast in the West London regions the decrease in benzene to toluene ratios, corresponding to fresh emissions and younger air masses, is coupled to a decrease of the O_3/NO_x suggesting ozone titration processes as expected and explained previously. The correlation coefficient R between the O_3/NO_x and the toluene to benzene ratio is of about 0.76.

4.3 Ozone budget

As illustrated in the Introduction, the diurnal ozone production can be evaluated studying which termination of the reactions cycle (R1)-(R7) is dominant between the reactions (R1)-(R2) (alkyl nitrate production) and (R1) (R3)-(R7) (ozone production). In our case study it is interesting to evaluate the ozone removal and production since the high concentrations of ΣANs measured suggest

that the HO_x-NO_x coupled reactions cycles leads to a marked production of *ΣANs* to the detriment of the ozone production.

The most significant mechanism of alkyl nitrate production is the reaction between RO_2 and *NO*; it is expected, therefore, that the *VOCs* and NO_x are well correlated with *ΣANs* when they are formed. We evaluated the correlation between the *ΣANs* and the NO_x and between *ΣANs* and different VOCs; in Fig.7 and Fig.8 we reported the results of the scatter plot between the *ΣANs* and NO_x and the toluene, selected for example. We found positive slopes and high correlation coefficients confirming, then, the significant process of alkyl nitrate production that characterized the urban and suburban area around London.

This is particularly true in the downwind regions (West London) where there are high concentrations of NO_x, locally produced (as above Reading) and transported (as suggested by the measured wind and the back trajectories analysis), demonstrating a reduction of the ozone production in favour of alkyl nitrate production.

Several studies investigated the ozone production (Cazorla et al., 2012; Farmer et al., 2011; Kleinman et al., 2005; Perring et al., 2010; Rosen et al., 2004) using different approaches. In our analysis we used the model adopted by Cazorla et al. (2012). In their study, Cazorla et al. (2012) measured the ozone production using a MOPS instrument and compared their measurements with the calculated production rate of ozone (via reactions between HO_2 and RO_2 and *NO*) and the modelled production rate of ozone (from a box model with the RACM2 mechanism); they found that the measured and calculated P_{O_3} had similar peaks with a temporal shift during the morning in the calculated P_{O_3} compared with the ozone production measured; the modelled, in contrast, was about half the measured production rate. In our analysis, we calculated the ozone net production as the difference between the production and the removal of ozone, following Cazorla et al. (2012):

$$P(O_3) = p(O_3) - l(O_3) \quad (6)$$

376 The production and removal ozone terms can be defined using the following kinetic equations:

$$p(O_3) = k_{HO_2+NO}[HO_2][NO] + \sum k_{RO_{2I}+NO}[RO_{2I}][NO] - P\left(\sum ANs\right) \quad (7)$$

$$l(O_3) = k_{OH+NO_2+M}[OH][NO_2][M] + k_{HO_2+O_3}[HO_2][O_3] \quad (8)$$

377

378 where $k_{HO_2+NO} = 3.3\times10^{-12}\exp(270/T)$, $k_{RO_{2I}+NO} = 2.6\times10^{-12}\exp(365/T)$, k_{OH+NO_2+M} has been
379 calculated as suggested in Sander et al. (2011), $k_{HO_2+O_3} = 1.0\times10^{-14}\exp(-490/T)$ (Sander et al.,
380 2011) and the $P\left(\sum ANs\right)$ term represents the alkyl nitrate production (see below). In order to
381 calculate the production of ozone (7), since RO_{2i} was not measured during the campaign, following
382 the assumption of Perring et al. (2010), we assumed that [RO_{2i}] ~HO_2] and that a generic RO_2
383 behaves as $C_2H_5O_2$, and thus the rate $k_{RO_{2I}+NO}$ was chosen accordingly (Bardwell et al., 2005).

384 The alkyl nitrate production has been evaluated as (Farmer et al., 2011; Perring et al., 2010; Rosen
385 et al., 2004):

$$P\left(\sum ANs\right) = \sum_i \alpha_i k_{OH+RH_i}[OH][VOCs] \quad (9)$$

386 where α_i is the nitrate branching ratio defined as $\alpha = k_{R2}/(k_{R2}+k_{R3})$ (Perring et al., 2010; Rosen et
387 al., 2004) where k_{R2} and k_{R3} are the reaction constants of the reactions (R2) and (R3) (production of
388 alkyl nitrate and of O_3 (via NO_2 production)), respectively. The mean *OH* concentration measured
389 by the FAGE during the M25 circuits (1.77×10^6 molecule cm^{-3}) was used in the calculation, which
390 was the approach taken for the photochemical air mass evaluation. In Table 1 we summarized the
391 branching ratios α_i, the *OH* rate constants and the *VOCs* concentrations used for the calculation of
392 the *ΣANs* production (9) and measured by the WAS-GC-FID instrument.

393 Calculating the ozone removal and production, we observed that the removal term $l(O_3)$ is on
394 average greater than the production term; in Fig. 9 (lower panel) is showed the ozone net production
395 during the diurnal flight B548: it is evident that the net production found is negative and that the

396 removal process is marked in the high NO_x region (solid circles - West London area with younger
397 air masses).

398

399 **Table 1.** The nitrate branching ratios α_i, the OH rate constants and the VOCs concentrations used
400 for the calculation of the ΣANs production (9) and measured by the WAS-GC-FID instrument.
401 Species reported in Italic are not measured during the campaign and estimate from previous
402 campaigns, see notes below.

VOCs	α_i	$\overline{\alpha_i}$	$k_{OH+VOCs}$ ($cm^3 molecule^{-1} s^{-1}$)	**Concentrations (ppt)**
Alkenes				
Ethene	0.0005	0.0086[a]	8.20×10^{-12}	735
Propene	0.021		2.63×10^{-11}	150
1-Butene	0.039		3.14×10^{-11}	41
Trans-2-butene	0.041		6.40×10^{-11}	5
Isoprene	0.07	0.15[a]	1.01×10^{-10}	66
Butadiene	0.04	0.11[a]	6.66×10^{-11}	25
Methylpropene	*0.012*		5.14×10^{-11}	*200*[b]
2-methyl-1-butene	*0.02*		6.07×10^{-11}	*100*[b]
3-methyl-1-butene	*0.056*		3.18×10^{-11}	*30*[b]
2-methyl-2-butene	*0.034*		8.69×10^{-11}	*130*[b]
c2-butene	*0.041*		5.64×10^{-11}	*50*[b]
t2-pentene	*0.064*		6.70×10^{-11}	*130*[b]
c2-pentene	*0.064*		6.50×10^{-11}	*60*[b]
Aromatics				
Benzene	0.029	0.10[a]	1.22×10^{-12}	638
Toluene	0.079	0.10[a]	5.96×10^{-12}	390
O-xylene	0.081	0.10[a]	1.36×10^{-11}	110
M-P-Xylene	0.08	0.10[a]	1.75×10^{-11}	281
Ethylbenzene	0.072	0.10[a]	7.00×10^{-12}	96
Propylbenzene	*0.093*		5.80×10^{-12}	*40*[c]
3-Ethyltoluene	*0.094*		1.86×10^{-11}	*90*[c]
4-Ethyltoluene	*0.137*		1.18×10^{-11}	*30*[c]
1,3,5-Trimethylbenzene	*0.127*		5.76×10^{-11}	*5*[c]
1,2,4-Trimethylbenzene	*0.105*		3.25×10^{-11}	*90*[c]
Alkanes				

Ethane	0.009	0.019[a]	2.58×10^{-13}	3960
Propane	0.036		1.10×10^{-12}	1308
n-Butane	0.083		2.54×10^{-12}	1181
i-Butane	0.027	0.255[a]	2.19×10^{-12}	640
i-Pentane	0.075	0.35[a]	3.90×10^{-12}	530
2-3 Methylpentane	0.110	0.14[a]	5.35×10^{-12}	230
Pentane	0.123		4.00×10^{-12}	250
Hexane	0.212		5.45×10^{-12}	87
Heptane	0.278		7.02×10^{-12}	56
Octane	0.346		8.71×10^{-12}	19
Cyclopentane	*0.10*		4.82×10^{-12} [d]	*190*[b]
Cyclohexane	*0.17*		6.96×10^{-12} [d]	*600*[b]
Methycyclohexane	*0.17*		9.43×10^{-12} [d]	*300*[b]
Nonane	*0.393*		9.99×10^{-12} [d]	*50*[b]
Decane	*0.417*		1.12×10^{-11} [d]	*55*[b]
Other				
Acetylene	0.04		1.1×10^{-12}	450

Notes.

[a] The higher branching ratios used to calculate the alkyl nitrates production and taken from Rosen et al. (2004)

[b] Species not measured during the campaign and estimate from the measurements done by Perring et al. (2010)

[c] Species not measured during the campaign and estimate from the measurements done by Rosen et a. (2004)

[d] Rate constants by Gennaco et al. (2012)

The ratio between the ozone production (7) and the alkyl nitrates production (9) ($P_{O_3}/P_{\Sigma ANs}$) gives information about the balance of the two possible terminations of the reaction system (R1)-(R7); flying above the M25 motorway we calculated the $P_{O_3}/P_{\Sigma ANs}$. The $P_{\Sigma ANs}$ term was calculated using the branching ratios α_i and the concentrations of the VOCs measured (see Table 1) in flight and we

found that the ratio $P_{O_3}/P_{\Sigma ANs}$ varies between 20 and 2. In detail, calculating the ratio in the London plume we estimated that $P_{O_3}/P_{\Sigma ANs} = 7$ (where the ozone production is 0.0385 ppt/s and the alkyl nitrates production is 0.0054 ppt/s). Calculating the contribution to the $P_{\Sigma ANs}$ of each class of *VOCs*, we found that they contribute almost for the same amount (36% Alkenes, 32% Alkanes, 31 Aromatics and 1% Acetylene). Moreover, the ratio between the ozone and the *ΣANs* production can be evaluated directly using the measured concentrations of these species as the correlation slope between the O_x (to take into account the ozone titration by *NO*) and the alkyl nitrates (Fig. 10). As illustrated above, analyzing the ratio of O_x and *ΣANs* it is possible to determine which is the dominant process between the production of O_x and the production of *ΣANs*. In Fig. 10 the dependence between O_x and *ΣANs* during the M25 circuits of the B548 flight is shown; also in this analysis it is possible identify two regimes: one for East, and another for West London. The negative slope (grey circles) corresponds to older and cleaner air (probably emitted before sunrise comparing its negative slope) with wind flowing from the North Sea (see Fig. 3); the positive one (black circles) corresponds to high NO_x and younger air in the downwind of London region (see Fig. 3). At least for these observations, the O_x vs *ΣANs* plot shows a slope of about 1 for the fresh, urban plumes air (lower than 7 hours older). This slope is the lowest compared to that observed in other megacities so far, as reported in Table 2, where the $P_{O_3}/P_{\Sigma ANs}$ at different sites is listed, as well. In order to explain the London plume discrepancy between the value found for the calculated $P_{O_3}/P_{\Sigma ANs}$ (about 7) and the measured $O_x/\Sigma ANs$ (about 1), we evaluated the alkyl nitrates production increasing the branching ratios of some *VOCs* from the average to the maximum value of α_i, according with the analysis of Rosen et al. (2004) and Perring et al. (2010). The values are listed in Table 1 and indicated as $\overline{\alpha_i}$. In this case we found that the $P_{O_3}/P_{\Sigma ANs}$ decreases to 4, suggesting that a possible underestimation of the branching ratio for these species can explain at least part of the disagreement between the calculated $P_{O_3}/P_{\Sigma ANs}$ and the observed $O_x/\Sigma ANs$. To take into account also

442 the contribution of some *VOCs* that we did not measure during the flight, we estimated the
443 $P_{\Sigma ANs}$ assuming for these *VOCs* the concentrations collected by Rosen et al. (2004) and Perring et al.
444 (2010) (these species are highlighted in Latin in the Table 1). This final simulation allows to reach a
445
446 **Table 2.** The O_x/ ΣANs and $P_{O_3}/P_{\Sigma ANs}$ ratios in different sites.

Site	O_x /ΣANs	$P_{O_3}/P_{\Sigma ANs}$	References
University of California-Blodgett Forest Research Station (UC-BFRS 2000-2001)	80	-	*Day et al., 2003*
Texas Air Quality Study (TexAQS-2000) Houston	29 (9-12 LT) – 41 (14-18 LT)	-	*Rosen et al., 2004*
Intercontinental Transport Experiment – Phase B (INTEX-B 2006) – Mexico city	17 (0-10 hr) – 90 (50 hr)	60 (0-10 hr)	*Perring et a., 2010*
Deepwater Horizon oil spill (2010) Gulf of Mexico	6.2 ÷ 7.9	8	*Neuman et al., 2012*
RONOCO (2010) London	~1	~7	*this study*

447
448 value of $P_{O_3}/P_{\Sigma ANs}$ of 2 (where the ozone production is 0.0385 ppt/s and the alkyl nitrates production
449 is 0.0162 ppt/s), which is significantly closer to the ratio between the productions obtained by the
450 direct measurements of the ozone and alkyl nitrates concentrations. Also in this case we evaluated
451 the role played by each *VOCs* to the production of alkyl nitrates: despite the contribution of the
452 Alkenes remain almost unvaried (35%), the Aromatics become less important (23%) in behalf of
453 the Alkanes (42%). This analysis suggests that the *VOCs* oxidation of the species measured and the
454 average values of α_i (Perring et al., 2010) are not sufficient to justify the $P_{O_3}/P_{\Sigma ANs} = 7$ versus
455 $O_x/\Sigma ANs$ = 1. This may be because we are not taking into account unmeasured *VOCs* that may

contribute to the alkyl nitrate production. In consequence, the term of the *ΣANs* production is underestimated and, therefore, the $P_{O_3}/P_{\Sigma ANs}$ overestimated. Using different and higher branching ratios for the alkyl nitrates ($\overline{\alpha_i}$) and including unmeasured *VOCs* allowed to estimate better the $P_{\Sigma ANs}$ and to reduce the discrepancy between measurements and calculations. In the Houston plume, Rosen et al. (2004) found that $P_{O_3}/P_{\Sigma ANs} = 45$, the difference between this value and the ratio found in the London plume is explained considering that the ozone production in Houston is about 50 times higher respect to the P_{O_3} in London and, on the contrary, the alkyl nitrate in Houston is only two times greater than the *ΣANs* production in the London plume. Moreover, analyzing the time series of NO_x, O_3 and *ΣANs* in Houston (Rosen et al., 2004), it is possible to verify the different scenarios existing between London and Houston. In London, in fact, we found that in correspondence of the high NO_x level, the ozone decreases significantly and the alkyl nitrates increases; in Houston, on the other hand, when the ozone and the alkyl nitrates increase the NO_x decreases. This is another indication of the different balance in the HO_x-NO_x reactions cycles between Houston and London, in the latter, during the observations flight reported here, the high NO_x emissions and the significant *VOCs* oxidation processes forming *ΣANs* involve a decrease in the ozone level.

5. Conclusions

In this paper we presented the results of a daytime flight (B548) along the M25 motorway around London. These observations confirm previous aircraft measurements of the pollutants species (NO_x and ozone) around London, in particular the presence of high NO_x concentrations above Reading (West London) (McMeeking et al., 2012). With the help of species not observed previously over London, like *ΣANs* , *ΣPNs* and HNO_3, here we had a chance to a deeper investigation of the chemistry in the London area and the high level of NO_x over Reading. In correspondence of those

plumes strong ozone titration processes and significant high *ΣANs* concentration are observed. The ozone and alkyl nitrate production analysis confirms that in the urban and suburban London area the alkyl nitrate production plays an important role affecting the ozone budget, at least during the day of observations reported here. The $P_{O_3}/P_{\Sigma ANs} = 7$, found calculating the alkyl nitrate production considering only the *VOCs* measured in the flight is significantly different respect to the observed $O_x/\Sigma ANs = 1$ that suggests a further study of the role played by the *VOCs* oxidation in the London plumes. From sensitivity tests, made increasing the branching ratios of some *VOCs* and taking into account the contribution of some unmeasured *VOCs*, we found that the calculated ratio $P_{O_3}/P_{\Sigma ANs}$ becomes 2, approaching notably the measured. This analysis suggests that attention must be paid on the branching ratio of *VOCs* and on the Alkanes that play an important role in the alkyl nitrate production in London affecting the local ozone production.

Acknowledgments

This work was performed within the RONOCO consortium supported by the Natural Environmental Research Council (NERC) (University of Cambridge grant award reference RG50086 MAAG/606, University of Leicester grant award reference E/F006761/1, University of East Anglia grant award reference NE/F005520/1). We thank Prof. Ron Cohen for stimulating discussions and inputs on this paper. We thank the Centre of Excellence CETEMPS for supporting this research and the FAAM, Avalon Aero and DirectFlight people for their essential assistance.

References

Bardwell, M. W., Bacak, A., Raventos, M. T., Percival, C.J., Sanchez-Reyna, G., Shallcross, D. E., 2005. Kinetics and mechanism of the $C_2H_5O_2$ + NO Reaction: a temperature and pressure dependence study using chemical ionisation mass spectrometry. International Journal of Chemical Kinetics 37(4), 253-260.

Cazorla, M., Brune, W.H., Ren, X., Lefer, B., 2012. Direct measurement of ozone production rates in Houston in 2009 and comparison with two estimation methods. Atmospheric Chemistry and Physics 12, 1203-1212.

Charron, A., Harrison, R.M., Quincey, P.. 2007. What are the sources and conditions responsible for exceedences of the 24h PM10 limit value (50 μg m^{-3}) at a heavily trafficked London site?. Atmospheric Environment 41, 1960-1975.

Commane, R., Floquet, C.F.A., Ingham, T., Stone, D., Evans, M.J., Heard, D. E., 2010. Observations of OH and HO2 radicals over West Africa. Atmospheric Chemistry and Physics 10, 8783-8801.

Dari-Salisburgo, C., Di Carlo, P., Giammaria, F., Kajii, Y., D'Altorio, A., 2009. Laser induced fluorescence instrument for NO2 measurements: Observations at a central Italy background site. Atmospheric Environment 43, 4, 970-977.

Day, A.D., Wooldridge, P.J., Dillon, M.B., Thornton, J.A., Cohen, R.C.. 2002. A thermal dissociation laser-induced fluorescence instrument for in situ detection of NO_2, peroxy nitrates, alkyl nitrates and HNO_3. Journal of Geophysical Research 107, No. D6,10.1029/2001JD000779.

Day, D. A., Dillon, M. B., Wooldridge, P.J., Thornton, J.A., Rosen, R.S., Wood, E.C., Cohen, R.C., 2003. On alkyl nitrates, O_3, and the "missing NO_y". Journal of Geophysical Research 108(D16), 4501, doi:10.1029/2003JD003685.

Di Carlo, P., Aruffo, E., Busilacchio, M., Giammaria, F., Dari-Salisburgo, C., Biancofiore, F., Visconti, G., Lee, J., Moller, S., Reeves, C. E., Bauguitte, S., Forster, G., Jones, R. L., Ouyang, B., 2013. Aircraft based four-channel thermal dissociation laser induced fluorescence instrument for simultaneous measurements of NO_2, total peroxy nitrate, total alkyl nitrate, and HNO_3. Atmospheric Measurements Technique 6, 971-980.

Draxler, R. R., Rolph, G.D., 2003. HYSPLIT (HYbrid Single-Particle Lagrangian Integrated Trajectory) Model. NOAA Air Resources Laboratory, Silver Spring, MD, available at: http: //www.arl.noaa.gov/ready/hysplit4.html.

European Environment Agency (EEA), 2005. Air pollution by ozone in Europe in summer 2004. Technical report 3/2005, Copenaghen, Denmark. (Available at http://reports.eea.eu.int).

Farmer, D.K , Perring, A. E., Wooldridge, P. J., Blake, D. R., Baker, A., Meinardi, S., Huey, L. G., Tanner, D., Vargas, O., Cohen, R. C., 2011. Impact of organic nitrates on urban ozone production. Atmospheric Chemistry and Physics 11, 4085–4094.

Gennaco, M.A., Huang, Y.W., Hannun, R. A., Dransfield, T.J., 2012. Absolute rate constants for the reaction of OH with cyclopentane and cycloheptane from 233 to 351 K. Journal of Physics and Chemistry A. 116 (51), 12438-43, doi: 10.1021/jp3048482.

Harrison, R.M., Dall'Osto, M., Beddows, D.C.S., Thorpe, A.J., Bloss, W.J., Allan, J.D., Coe, H., Dorsey, J.R., Gallagher, M., Martin, C., Whitehead, J., Williams, P.I., Jones, R.L., Langridge, J.M., Benton, A.K., Ball, S.M., Langford, B., Hewitt, C.N., Davison, B., Martin, D., Petersson, K.F., Henshaw, S.J., White, I.R., Shallcross, D.E., Barlow, J.F., Dunbar, T., Davies, F., Nemitz, E., Phillips, G.J., Helfter, C., Di Marco, C.F., Smith, S., 2012. Atmospheric chemistry and physics in the atmosphere of a developed megacity (London): an overview of the REPARTEE experiment and its conclusions. Atmospheric Chemistry and Physics 12, 3065-3114.

Hopkins, J. R., Lewis, A.C. , Read, K.A., 2002. A two-columnmethod for long-term monitoring of non-methane hydrocarbons (NMHCs) and oxygenated volatile organic compounds (o-VOCs). Journal of Environmental Monitoring 4, 1–7.

Hopkins, J. R., Jones, C.E., Lewis, A.C., 2011. A dual channel gas chromatograph for atmospheric analysis of volatile organic compounds including oxygenated and monoterpene compounds. Journal of Environmental Monitoring, doi:10.1039/c1em10050e.

Jacob, D. J., 1999. Introduction to atmospheric chemistry, Princeton University Press, Princeton, New Jersey.

Kleinman, L.I., Daum, P. H., Lee, Y.-N., Nunnermacker, L. J., Springston, S. R., Weinstein-Lloyd, J., Hyde, P., Doskey, P., Rudolph, J., Fast, J., Berkowitz, C., 2003. Photochemical age determinations in the Phoenix metropolitan area. Journal of Geophysical Research 108(D3), 4096, doi:10.1029/2002JD002621.

Kleinman, L.I., 2005. The dependence of tropospheric ozone production rate on ozone precursors. Atmospheric Environment 39, 575-586.

Kleinman, L.I., Springston, S.R., Daum, P.H., Lee, Y.-N., Nunnermacker, L.J., Senum, G.I., Wang, J., Weinstein-Lloyd, J., Alexander, M.L., Hubbe, J.. Ortega, J., Canagaratna, M.R., Jayne, J., 2008. The time evolution of aerosol composition over the Mexico City plateau. Atmospheric Chemistry and Physics 8, 1559-1575.

Langford, B., Nemitz, E., House, E., Phillips, G.J., Famulari, D., Davison, B., Hopkins, J.R., Lewis, A.C., Hewitt, C.N., 2010. Fluxes and concentrations of volatile organic compounds above central London, UK. Atmospheric Chemistry and Physics 10, 627-645.

Le Breton, M., McGillen, M., Muller, J.B.A., Bacak, A., Shallcross, D.E., Xioa, P., Huey, L.G., Tanner, D., Coe, H., Percival, C.J., 2012. Airborne observations of formic acid using a chemical ionisation mass spectrometer. Atmospheric Measurement Techniques 4, 3029-3039.

Liggio, J., Li, S.-M., Vlasenko, A., Sjostedt, S., Chang, R., Shantz, N., Abbatt, J., Slowik, J.G., Bottenheim, J. W., Brickell, P.C., Stroud, C., Leaitch, W.R., 2010. Primary and secondary organic aerosols in urban air masses intercepted at a rural site. Journal of Geophysical Research 115, D21305, doi:10.1029/2010JD014426.

McMeeking, G.R., Bart, M., Chazette, P., Haywood, J.M., Hopkins, J.R., McQuaid, J.B., Morgan, W.T., Raut, J.-C., Ryder, C.L., Savage, N., Turnbull, K., Coe, H., 2012. Airborne measurements of trace gases and aerosols over the London metropolitan region Atmospheric Chemistry and Physics 12, 5163-5187.

Neuman, J.A., Aikin, K.C., Atlas, E.L., Blake, D.R., Holloway, J.S., Meinardi, S., Nowak, J.B., Parrish, D.D., Peischl, J., Perring, A.E., Pollack, I.B., Roberts, J.M., Ryerson, T.B., Trainer, M., 2012. Ozone and alkyl nitrate formation from Deepwater Horizon oil spill atmospheric emissions. Journal of Geophysical Research 117, D09305, doi:10.1029/2011JD017150.

Perring, A.E., Bertram, T.H., Farmer, D.K., Wooldridge, P.J., Dibb, J., Blake, N.J., Blake, D.R., Singh, H.B., Fuelberg, H., Diskin, G.,. Sachse, G., Cohen, R.C., 2010. The production and persistence of ΣRONO2 in the Mexico City plume. Atmospheric Chemistry and Physics 10, 7215-7229.

Rosen, R.S., Wood, E.C., Wooldridge, P.J., Thornton, J.A., Day, D.A., Kuster, W., Williams, E.J., Jobson, B.T., Cohen, R.C., 2004. Observations of total alkyl nitrates during the Texas Air Quality Study 2000: Implications for O3 and alkyl nitrates photochemistry. Journal of Geophysical Research 109, D07303, doi:10.1029/2003JD004227.

Sadanaga, Y., Fukumori, Y., Kobashi, T., Nagata, M., Takenaka, N., Bandow, H., 2010. Development of a Selective Light-Emitting Diode Photolytic NO_2 converter for continuously measuring NO_2 in the atmosphere. Analytical Chemistry 82, 9234-9239.

Sander, S.P., Barker, J.R., Golden, D.M., Kurylo, M.J., Wine, P.H., Abbatt, J.P.D., Burkholder, J.B., Kolb, C.E., Moortgat, G.K., Huie, R.E., 2011. Chemical Kinetics and Photochemical Data for use in atmospheric Studies. JPL Publication 17.

Slowik, J.G., Brook, J., Chang, R. Y.-W., Evans, G.J., Hayden, K., Jeong, C.-H., Li, S.-M., Liggio, J., Liu, P.S.K., McGuire, M., Mihele, C., Sjostedt, S., Vlasenko, A., Abbatt, J.P.D., 2011. Phochemical processing of organic aerosol at nearby continental sites: contrast between urban plumes and regional aerosol. Atmospheric Chemistry and Physics 11, 2991-3006.

Stone, D., Evans, M.J., Edwards, P.M., Commane, R. Ingham, T., Rickard, A.R., Brookes, D.M., Hopkins, J., Leigh, R.J., Lewis, A.C., Monks, P.S., Oram, D., Reeves, C.E., Stewart, D., Heard, D.E., 2011. Isoprene oxidation mechanisms: measurements and modeling of OH and HO_2 over a South-East Asian tropical rainforest during the OP3 field campaign. Atmospheric Chemistry and Physics 11, 6749-6771.

Stone, D., Evans, M.J., Walker, H.M., Ingham, T., Vaughan, S., Ouyang, B., Kennedy, O.J., McLeod, M.W., Jones, R.L., Hopkins, J., Punjabi, S., Lidster, R., Hamilton, J.F., Lee, J.D., Lewis, A.C., Carpenter, L.J., Forster, G., Oram, D.E., Reeves, C.E., Baugitte, S., Morgan, W., Coe., H., Aruffo, E., Dari-Salisburgo, C., Giammaria, F., Di Carlo, P., Heard D.E., 2013. Radical chemistry at night: comparisons between observed and modelled HO_x, NO_3 and N_2O_5 during the RONOCO project. Atmospheric Chemistry and Physics Discussion 13, 9519-9566.

Von Bobrutzki, K., Braban, C.F., Famulari, D., Jones, S.K., Blackall, T., Smith, T.E.L., Blom, M., Coe, H., Gallagher, M., Ghalaieny, M., McGillen, M.R., Percival, C.J., Whitehead, J.D., Ellis, R., Murphy, J., Mohacsi, A., Pogany, A., Junninen, H., Rantanen, S., Sutton, M.A., Nemitz E., 2010. Field inter-comparison eleven atmospheric ammonia measurement techniques. Atmospheric Measurements Technique 3, 91-112.

Figures captions

Fig. 1. B548 flight paths. The colour bar identifies the altitude; the capital letters indicate two airports (Southend (S) and Northolt (N)), the city of London (L) and Reading (R). The black lines represent the UK coast.

Fig. 2. B548 flight time series (the time is expressed in seconds after midnight, sec. A.M.). The green line represents the altitude and the grey square identify the M25 London circuit.

Fig. 3. On top: NO_2 (the colorbars on the right sides indicated the concentrations levels in ppbv) measured on flight during the three M25 circuits at 11:00 UTC, 12:00 UTC and 13:00 UTC, respectively. Bottom: the wind direction along the flight trajectory (grey arrows) and the NO_2 concentrations (colorbars on the right sides indicate the level in ppbv) measured in three ground stations (R = Reading, H = Haringey and L = London).

Fig. 4. On top: the $-\ln([NO_x]_t/[NO_y])$ term of the equation (2) in the West and East London regions. At the bottom: the photochemical ages (hr) in the West and East London regions.

Fig. 5. On top: trends of the concentration of NO_x, ΣPNs, ΣANs and HNO_3 measured along the M25 motorway as function of the photochemical age. At the bottom: the dependence of the NO_y speciation from the photochemical age.

Fig. 6. Benzene to toluene ratio and the O_3/NO_x during the B548 flight.

Fig. 7. Scatter plot between alkyl nitrates and NO_x. The grey points identify the East London plumes, the black points the London/Reading urban plumes. The linear fit and the correlation coefficients have been calculated for all the data.

Fig. 8. Scatter plot between alkyl nitrates and toluene. The grey points identify the East London plumes, the black points the London/Reading urban plumes. The linear fit and the correlation coefficients have been calculated for all the data.

Fig. 9. At the top: the ozone production (black asterisk) and loss (black square) during the B548 diurnal flight calculated by equations (7) and (8), respectively. At the bottom: the net ozone production calculated for the diurnal flight B548: open circles identify the East London region (low NO_x, more aged air), solid circles identify the West London region (high NO_x, less aged air).

Fig. 10. The relation between O_x and ΣANs: we found two regimes (East London in grey points – West London in black points).

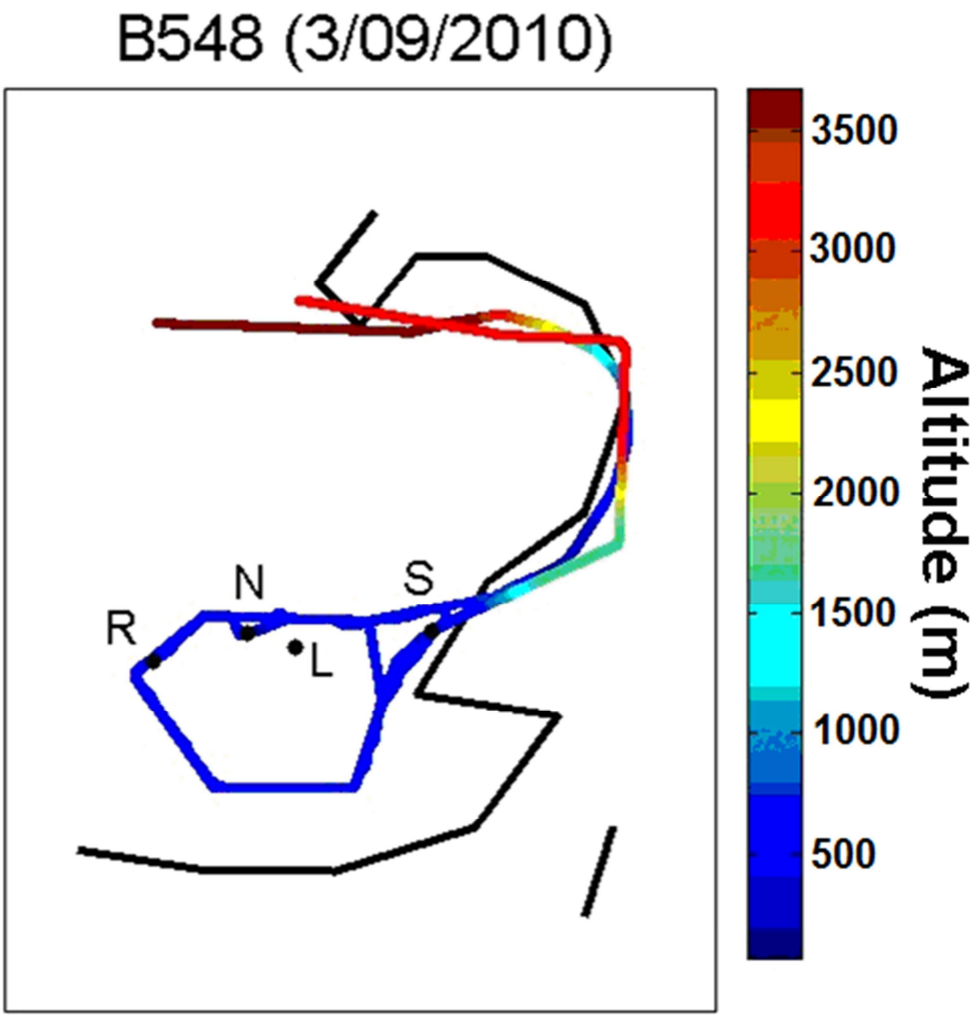

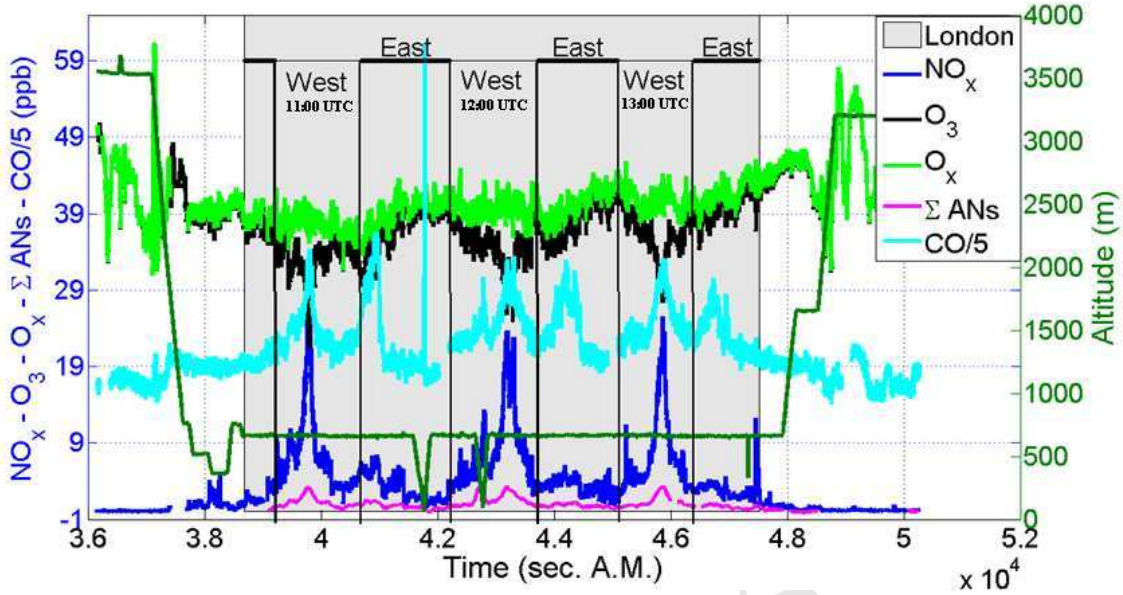

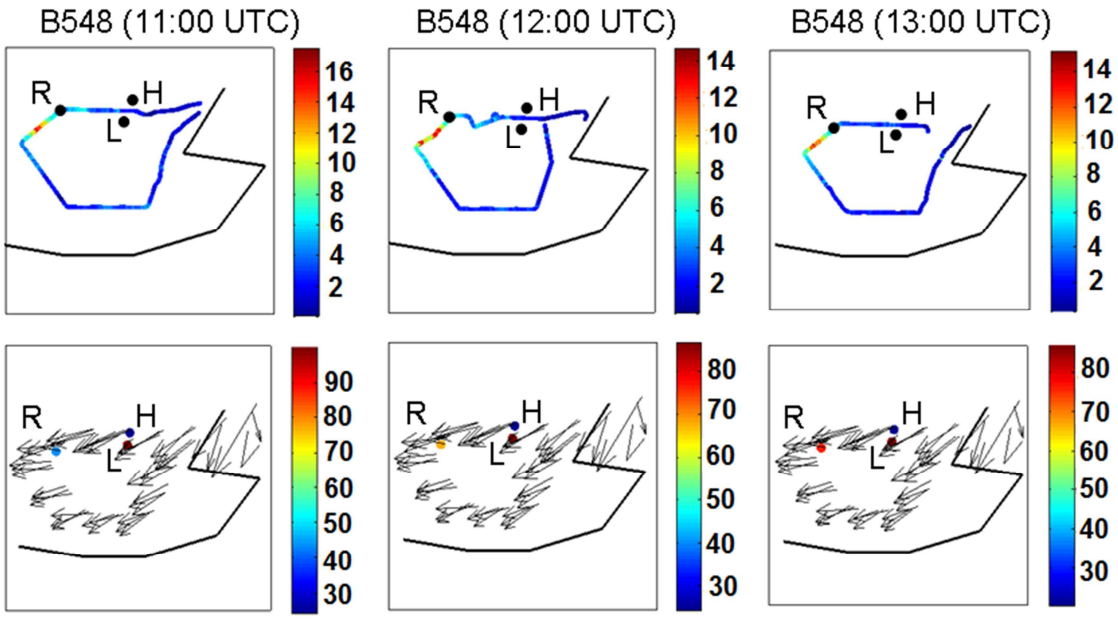

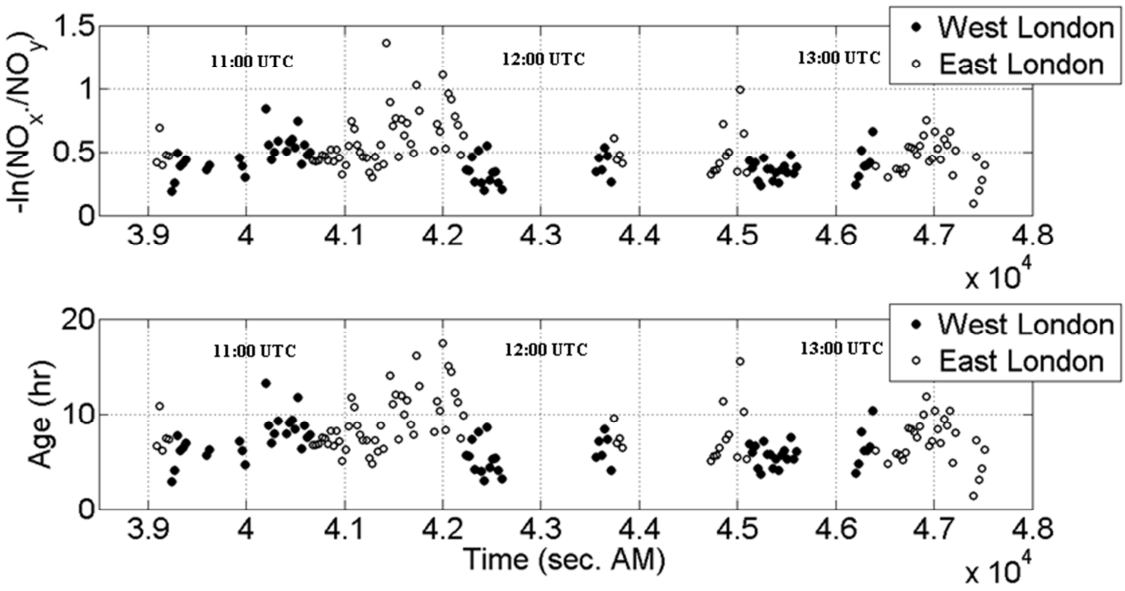

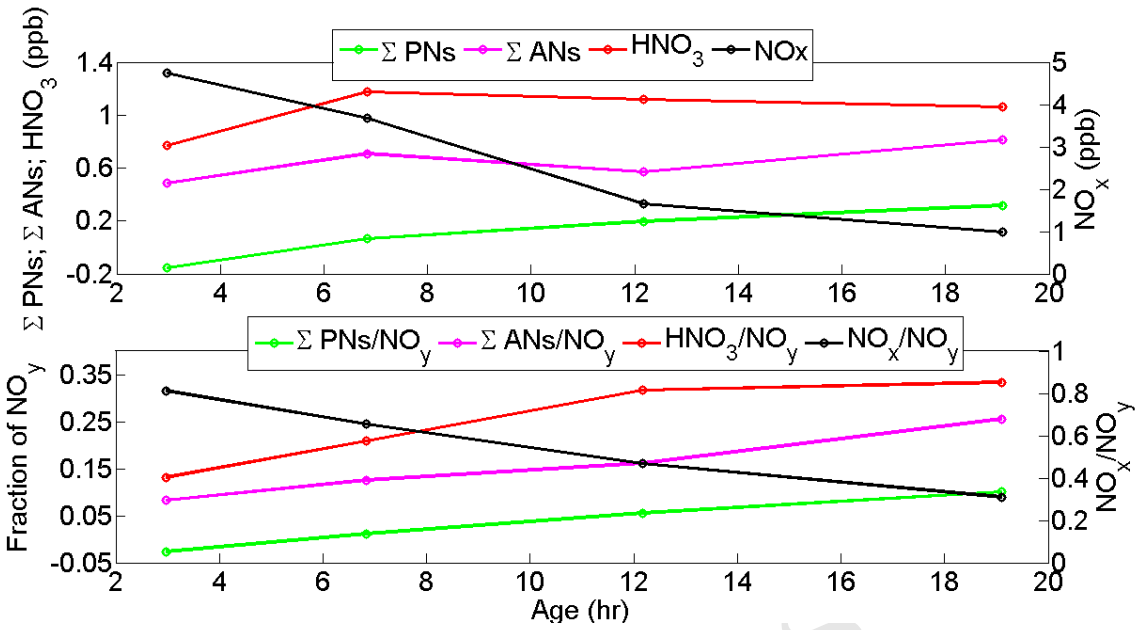

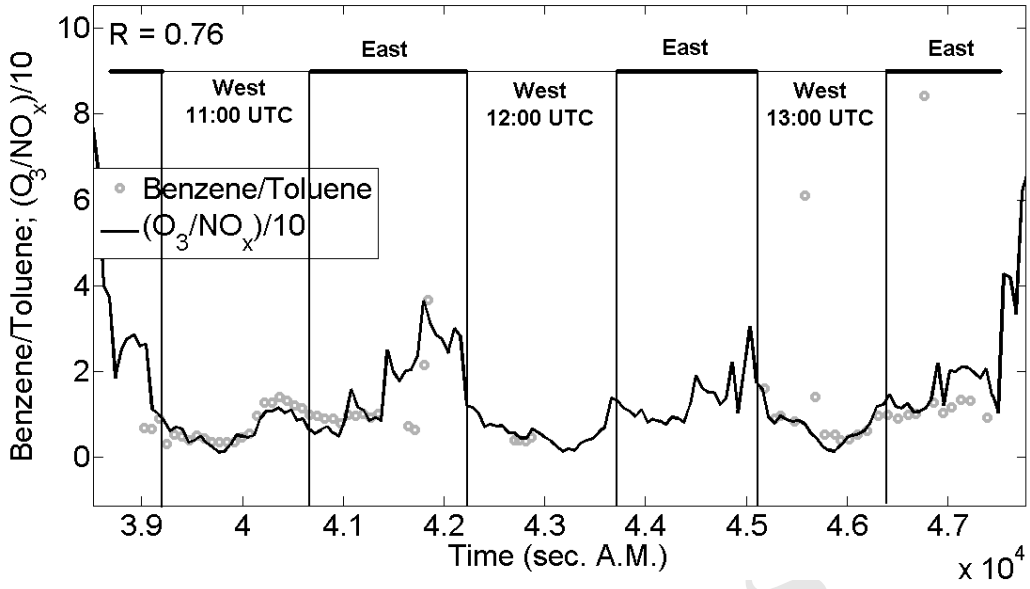

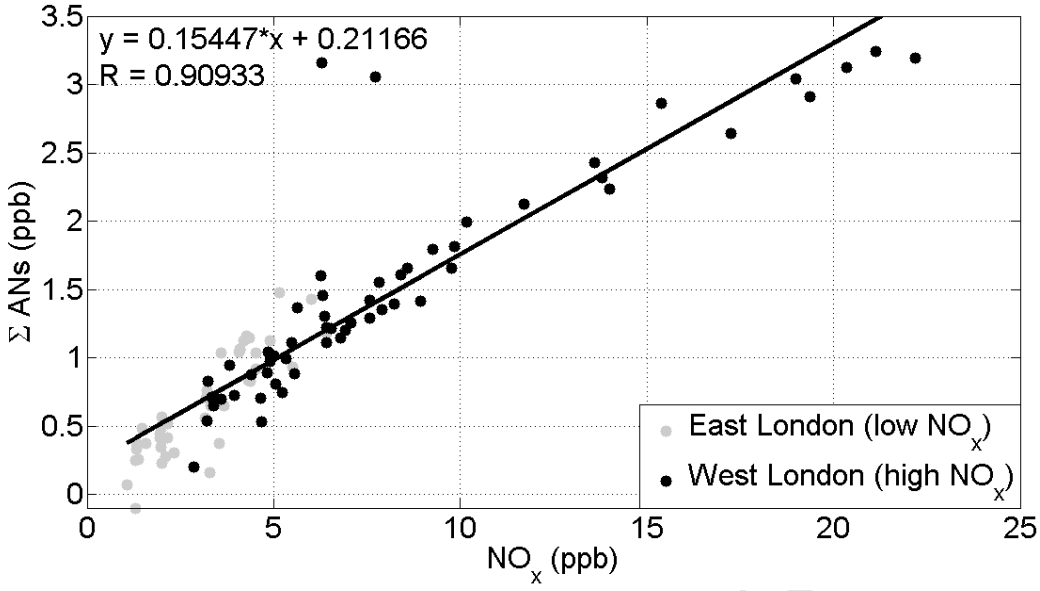

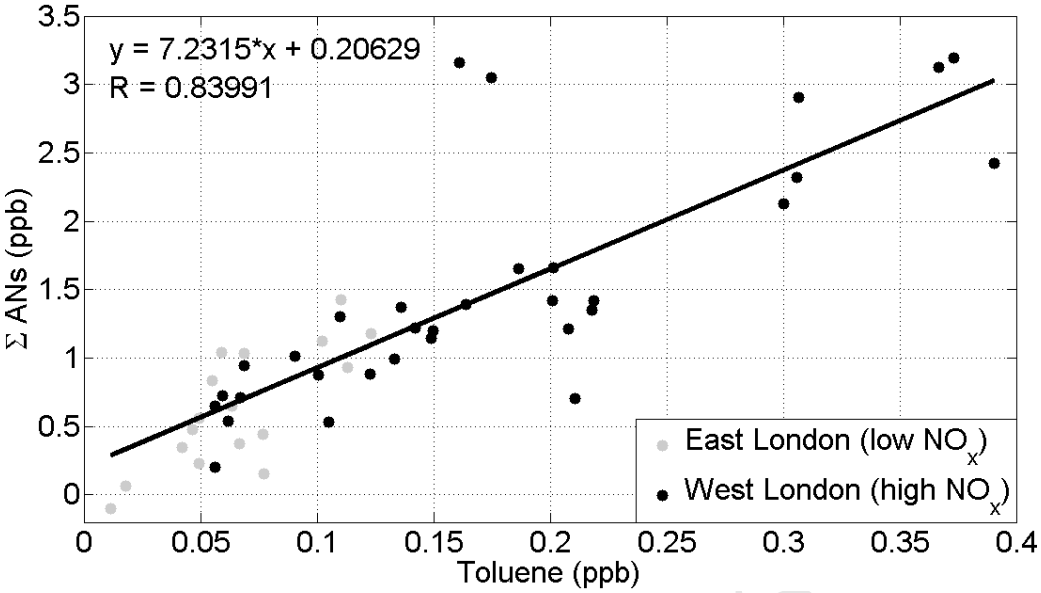

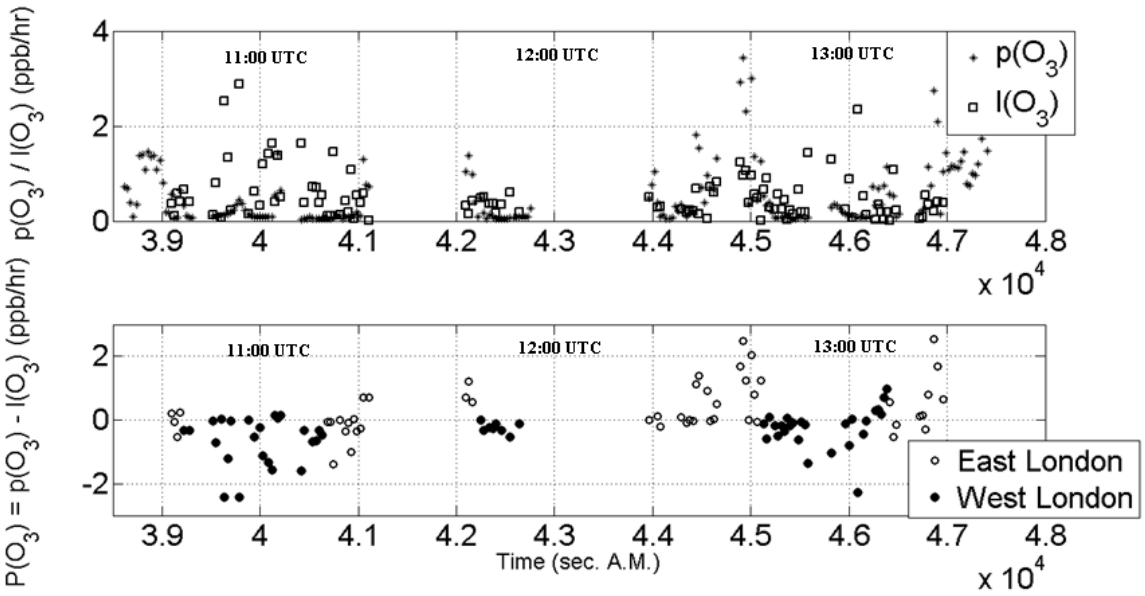

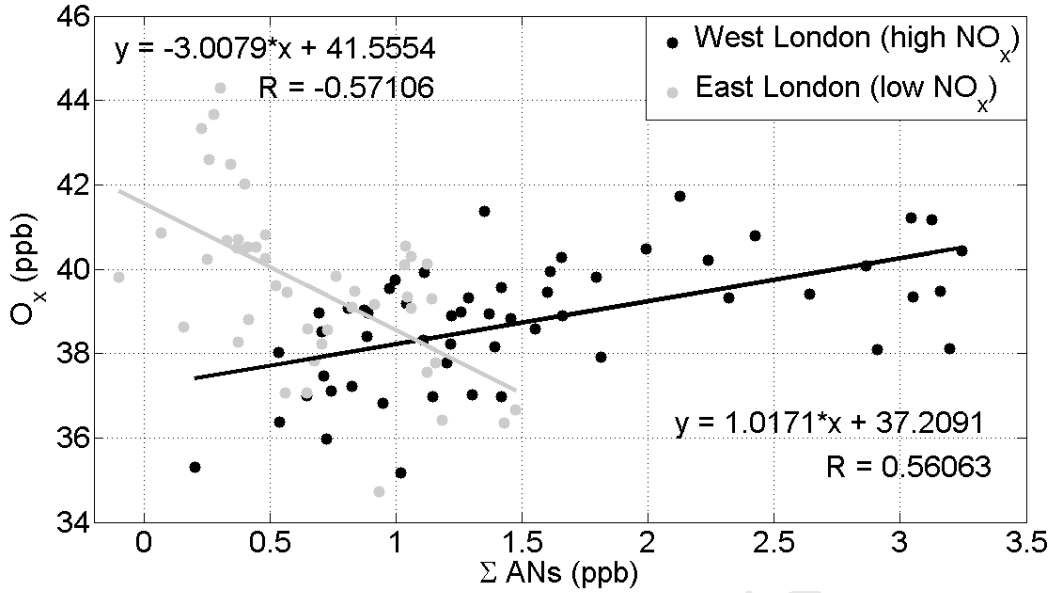

Highlights

- Daytime chemical and aerosol composition have been measured around London with an aircraft
- Unexpected high production of alkyl nitrate comparable to that of ozone
- The low O_3 production put the chemistry above London quite different compared with other megacities